

Qualitative and quantitative interpretation of high-resolution gravity data of Ewekoro, Southwest Nigeria using source parameter imaging and Euler deconvolution techniques

Gideon Oluyinka Layade^{1*}, Emmanuel Oluwatoyin Bamidele², Victor Makinde³, Babatunde Saheed Bada⁴
and Hazeen Owolabi Edunjobi⁵

¹ Associate Professor, Department of Physics, (Geophysics Unit), Federal University of Agriculture, Abeokuta, Nigeria

² M.Sc Graduate, Department of Physics, Federal University of Agriculture Abeokuta, Nigeria

³ Professor, Department of Physics, (Geophysics Unit) Federal University of Agriculture Abeokuta, Nigeria

⁴ Professor, Department of Environmental Management & Toxicology, Federal University of Agriculture Abeokuta, Nigeria

⁵ Lecturer, Department of Physics, Sikiru Adetona College of Education, Science and Technology, Omu-Ajose, Nigeria

(Received: 31 July 2023, Accepted: 23 December 2023)

Abstract

Geoscientists are interested in investigating the subsurface mineral resources such as crude oil through exploration of the Earth's subsurface. The availability and extent of these important commercial minerals can be ascertained by the characteristics of their geophysical properties through a geophysical survey in the area under investigation. Gravity method is a non-destructive geophysical method primarily used for locating the presence of solid minerals. This research work is aimed at using data coordinate interpolation techniques to extract information from aerogravity data obtained over Ewekoro in order to estimate the depth of the overburden thickness of the geological contact of the observed causative potential field anomaly. Hence, Source Parameter Imaging (SPI) and Euler deconvolution methods were applied on airborne gravity data of Ewekoro in both qualitative and quantitative approaches. The airborne gravity data sheets 260 and 279 acquired by the Bureau Gravimetric International (BGI), through the Earth Gravity Model (EGM08) in 2008 were used. The raw gravity data recorded in digital format of X, Y and Z representing latitude, longitude and the Bouguer gravity values, respectively, were exported into Oasis Montaj software for qualitative and quantitative analysis. The datasets were gridded using the minimum curvature algorithm. Regional-residual separation was carried out to remove low frequency anomalies from the total field by applying a high-pass filter in sharpening the edges of the anomaly and enhancement. A Two-Dimensional Fast Fourier Transform (2D FFT) filtering technique was used in computing different derivative grids. The interpolated gravity map revealed a decrease in anomaly from SW to NE of the study area, with an anomaly range of 15–19 mGal. The SPI revealed a depth range of 235–698 m with the deeper gravity source concentrated in the central region and shallower source discovered in the SE of the study area. The 3D Euler depth estimates corresponding to Structural Index (SI) = 0 applied to the gravity data revealed a depth range of 132–692 m with a scattered Euler solution trending in NW, NE and SSE of the study area. The results for both methods indicate an average correlation in terms of their depths. The investigation revealed Bouguer anomaly thickness of Ewekoro trends in the SW–NE with significant depth for mineral exploration. The heterogeneity of the subsurface of the study area and the overburden thickness of Ewekoro trending in the NNE–NNW with an appreciable depth to harbour mineral resources were established.

Keywords: Potential field, gravity, Bouguer, mineral, depth

1 Introduction

Being used globally, gravity survey is a passive, non-invasive and less expensive method (Rivas, 2009). This method measures the Earth's force of gravity at a particular study area with a view to identifying variations arising from anomalous causative body existing within the Earth and various host rock types (Sheriff, 2002). The gravity method is the most extensively adopted geophysical method for oil and gas (hydrocarbon) exploration, regional geological studies, detection of subsurface cavities (microgravity), location of buried rock-valley, exploration and mass estimation of mineral deposit, geodesy, volcanoes monitoring and isotactic geological studies in the twentieth century (Reynolds, 1997; Layade et al., 2021b). Two gravity force components are vital during gravity measurement. They are the general and relatively uniform component which can be measured in different platforms, such as air, land and sea but of all these measurement platforms, land surface presents the best platform in terms of the stability of the measuring instrument, reliability of data control over the measurement and its high resolution and precision (Osazuwa, 2014). Gravimeter is an instrument used in gravity exploration examples of which are LaCoste-Romberg gravimeter, Wordon gravimeter and Autograv CG-5 gravimeter. Nabighian et al. (2005) described gravitimeter as either absolute or relative. Gravity between successive measurements is done through relative gravitimeter, while absolute gravimeter measures the true value of gravity for every measurement. Gravity survey identifies variations in rock density. These variations are based on how accessible subsurface rock is as a result of geophysical processes, such as weathering and dehydration, where they are subjected to mechanical stress from cracking as opposed to when in situ

(Reynolds, 1997). The difference between the measured field and the local field of different density contrast of the source body is the gravitational causative body (Kearey et al., 2002; Layade et al., 2021a). Applied geophysicists and geologists were intrigued by the relationship between the Bouguer anomaly and the lateral variation in upper crustal density obtained through gravity data reduction. The Bouguer anomaly is the difference between the gravity value of the base station and that obtained after necessary reduction. Thus, it is essential that the Bouguer anomaly variation captures the lateral density contrast of both positive and negative Bouguer anomaly (Layade, et al., 2020; Rivas, 2009). However, other physical properties that are of concern to geophysicists as outlined by Bonde et al. (2014) are electrical conductivity (or resistivity), dielectric permittivity, natural radioactivity, thermal conductivity and acoustic velocity among others.

The law of universal gravitation and second law of motion derived by Newton are fundamental in gravity theory derivations as affirmed by Reynolds (1997). The law of universal gravitation states that the attractive force existing between two bodies of masses (M) and (m) is directly proportional to the product of the two masses and inversely proportional to the square of their distance of separation. This is mathematically expressed as:

$$F = \frac{GMm}{R^2} \quad (1)$$

where

F = attractive force between two bodies;
 G = gravity constant ($G = 6.67 \times 10^{-11} \text{ Nm}^2/\text{kg}^2$);
 M = mass of the Earth;
 m = mass of the second body;
 R = distance of separation.

It can be deduced from Newton's second law of motion that the product of the mass of a body and its acceleration is equal to the force applied. Basically, for

acceleration due to gravity, it is vertically directed towards the Earth's surface. Theoretically, this law is given as:

$$F = \frac{dp}{dt} \quad (2)$$

Therefore,

$$F = \frac{d(mv)}{dt} = mg \quad (3)$$

where

F = force of attraction;

dp = change in momentum;

dt = change in time.

Relating Eqs. (1) and (3), we obtain:

$$g = G \frac{M}{R^2} \quad (4)$$

From Eq. (4) it can be stated that the magnitude of the Earth's gravitational acceleration is a function of its mass and the inverse of the square of the Earth's radius (R). Though gravitational acceleration should theoretically be constant over the Earth, in reality it varies because the distribution of the mass of the Earth from place to place changes and surface topography (shape of the Earth) is irregular.

2 Study area

2-1 Description of the study area

Ewekoro can be found specifically within latitudes $6^{\circ}53'30''$ to $6^{\circ}57'30''$ and longitudes $3^{\circ}11'30''$ to $3^{\circ}14'30''$, in the Ewekoro Local Government Area Ogun State, Nigeria. Adejuwon and Adedokun, (2012) stated that Ewekoro is bordered by the local government areas of Obafemi Owode in the west, Yewa North and Yewa South in the east, Ifo Local Government Area in the south, and Abeokuta North and Abeokuta South in the north. It is located in subequatorial southwest tropical rain forest of Nigeria. Oladosu and Ogundipe (2017) asserted that Ewekoro is characterized by two distinct seasons of the climate in Nigeria in a year. The average mean annual rainfall and mean monthly temperature are between 1500-2000 mm and 22°C - 22.5°C , respectively. The average relative humidity of the area under consideration

is between 75 and 95 percent. In addition to having considerable limestone reserves, Ewekoro is home to a cement mill that belongs to Lafarge Africa. Predominantly, agricultural farming of cocoa, maize, and cocoyam is another economic boom in the area.

2-2 Geology of the study area

Ogun State is composed of sedimentary and basement complex rocks. It also contains argillaceous sediment intercalations. Despite being soft and friable, the rock has been cemented by ferruginous and siliceous substances in some places. Sedimentary rock in Ogun State is found in the Abeokuta Formation situated close above the basement complex. This is followed by the Ewekoro, Oshosun, and Ilaro Formations (Olurin et al., 2012). The Ewekoro Formation is made up of fossiliferous well-bedded limestone, whereas the Akinbo and Oshosun Formations are made up of hazy grey and black shales. Phosphatic beds and glauconitic rock bands divide the Ewekoro and Akinbo Formations. The majority of the layers in the Ilaro and Benin Formations are estuarine, deltaic, and continental, according to Oli et al. (2019). As specified by Oladosu and Ogundipe (2017), the sediments in the Tertiary formations Ewekoro, Akinbo, and others were deposited in both marine and transitional habitats, and their ages span from the Paleocene-middle to upper Eocene. The Cretaceous deposits of Dahomey basin are partially cut off from the Niger Delta strata which previously supported the ages assigned to the sequences. The establishment of Ewekoro proved to be financially significant because quarries used to make cement were located there and used by Lafarge (West African Portland Cement Company), Ewekoro, and Dangote Group Cement Company.

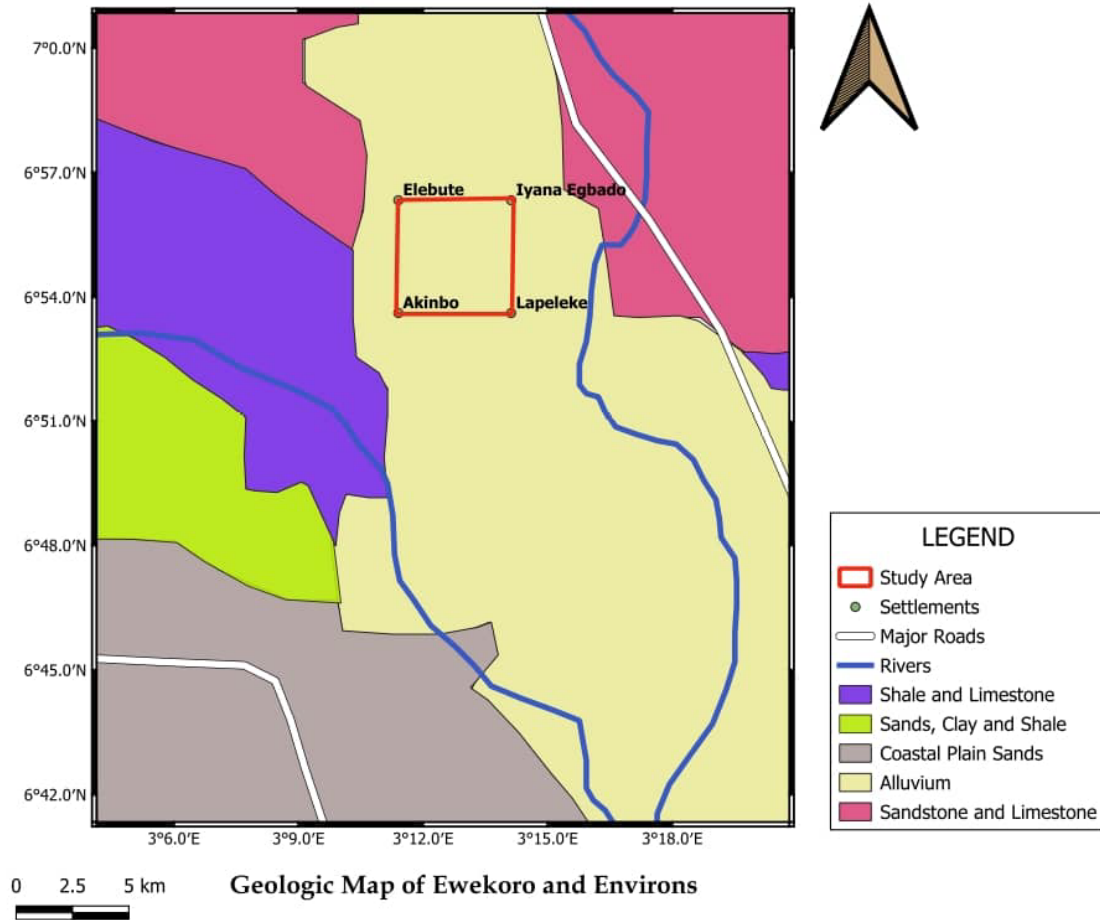


Figure 1. Geologic map of the study area.

3 Material and methods

3-1 Data source

The airborne gravity data (satellite-based data) sheets 260 and 279 acquired by the Bureau Gravimetric International (BGI), through the Earth Gravity Model (EGM08) in 2008 were used. The raw gravity data were recorded in digital format of X, Y and Z representing longitude, latitude and the Bouguer gravity values, respectively, exported into Oasis Montaj software for qualitative and quantitative analysis. The dataset was gridded using minimum curvature algorithm. Regional and residual separation and filtering were applied to enhance the gridded data.

3-2 Theoretical background for depth estimation methods

3-2-1 Source Parameter Imaging (SPI)

The Source Parameter Imaging method (Thurston and Smith, 1997; Nwosu, 2014; Ngozi et al., 2019; Layade et al., 2020) extends the complex analytical signal to estimate magnetic depths. The local wave number approach developed by Thurston and Smith (1997) is a grid- or profile-based method for calculating the depth of a magnetic source as well as its dip and susceptibility contrast for some source geometries. The technique makes use of the link between source depth and the local wave number (K) of the observed field, which can be estimated for every location within a data grid using horizontal and vertical gradients. An image is used to represent the depth. The SPI approach needs both first- and second-order derivatives making it susceptible to interference or noise in the data. This method was used by Thurston and Smith (1997) for sloping

contact 2-D and a 2-D dipping thin sheet. Nabighian (1972) expressed the analytic signal $A(x, z)$ as:

$$A(x, z) = \frac{\partial M(x, z)}{\partial x} - j \frac{\partial M(x, z)}{\partial z} \quad (5)$$

where

$M(x, z)$ is the magnitude of the anomalous total magnetic field;

j is the complex number;

z and x are Cartesian coordinates for the vertical direction and horizontal direction perpendicular to strike, respectively.

Nabighian (1972) showed the relationship between the horizontal and vertical derivatives that make up the real and imaginary sections of the 2D analytical signal is:

$$\frac{\partial M(x, z)}{\partial x} \Leftrightarrow -j \frac{\partial M(x, z)}{\partial z} \quad (6)$$

where \Leftrightarrow represents the Hilbert's transform pair.

The local wavenumber is defined by Thourston and Smith (1997) as:

$$K_1 = \frac{\partial}{\partial x} \tan^{-1} \left[\frac{\partial M}{\partial z} / \frac{\partial M}{\partial x} \right] \quad (7)$$

Expression for second order analytic signal is given by:

$$A_2(x, z) = \frac{\partial^2 M(x, z)}{\partial z \partial x} j \frac{\partial M(x, z)}{\partial^2 z} \quad (8)$$

Eq. (8) invariably gives rise to a second order local wave number K_2 :

$$K_2 = \frac{\partial}{\partial x} \tan^{-1} \left[\frac{\partial^2 M}{\partial^2 z} / \frac{\partial^2 M}{\partial z \partial x} \right] \quad (9)$$

3-2-2 Euler Deconvolution Method (EDM)

Euler deconvolution technique is used to estimate the source depth locations of the gravity or magnetic signature in a specific region (Thompson, 1982). The method

uses first-order x , y , and z derivatives to establish the position and depth of numerous idealized targets, such as spheres, cylinders, narrow dikes and contacts, each of which is distinguished by a unique structural index. The technique theoretically resolves the effect of overlapping edges, although it is mostly relevant to a few body types with established constant structural indices (Reid et al., 1990; Adegoke and Layade, 2019). Its application on gridded data and profiles provide solution to the Euler's homogeneity equation which is expressed as:

$$(x - x_0) \frac{df}{dx} + (y - y_0) \frac{df}{dy} + (z - z_0) \frac{df}{dz} = N(B - F) \quad (10)$$

where

$\frac{df}{dx}$, $\frac{df}{dy}$, and $\frac{df}{dz}$ denote the first-order derivatives;

x_0 , y_0 , and z_0 are source depth locations whose gravity and total field F are detected at x , y and z ;

B is the regional value of the field;

N is the Euler's structural index (SI) which is a function of the source geometry of the causative bodies.

The estimation of the source depth is based on application of the Euler deconvolution on the gridded data to provide solution to Euler's homogeneity equation which depends on the variation of the structural index. Table 1 shows variation in structural index (SI) values for gravity and magnetic models.

Table 1. Structural index values for different models.

Model	Magnetic SI	Gravity SI
point, sphere	3	2
line, cylinder, thin bed fault	2	1
thin sheet edge, thin sill, thin dyke	1	0
thick sheet edge ^a	0 ^a	-1 ^a
contact of infinite depth extent	0	not useful ^b

^a Requires the extended definition of SI as proposed by Stavrev and Reid (2007) and a non-linear deconvolution process.

^b The gravity anomaly is infinite [source: Reid et al. (2014)].

4 Results and discussion

4-1 Qualitative interpretation

Having channels representing the longitude, latitude and Bouguer gravity values, the digitized gravity dataset of sheets 260 and 279 of the BGI was exported into the Oasis Montaj software for analysis and qualitative and quantitative interpretation. The dataset was gridded using the minimum curvature algorithm. The gridded dataset produced the Bouguer anomaly map (Figure 2) which revealed a gravimetric range of 10 mGal to 39 mGal across the Ewekoro sheet with regions of high (pink

and red) and low (blue) gravity values observed all over the study area. The Bouguer anomaly grid in Figure 2 is made up of both long-wavelength low frequency anomaly and the short wavelength high frequency anomaly of the total field.

A regional-residual separation on the Bouguer anomaly grid was carried out. The Radially Averaged Power Spectrum (RAPS) (Figure 3) was generated using the Bouguer gravity anomaly grid to visualize long and short wavelength anomaly sources whilst revealing possible noise levels.

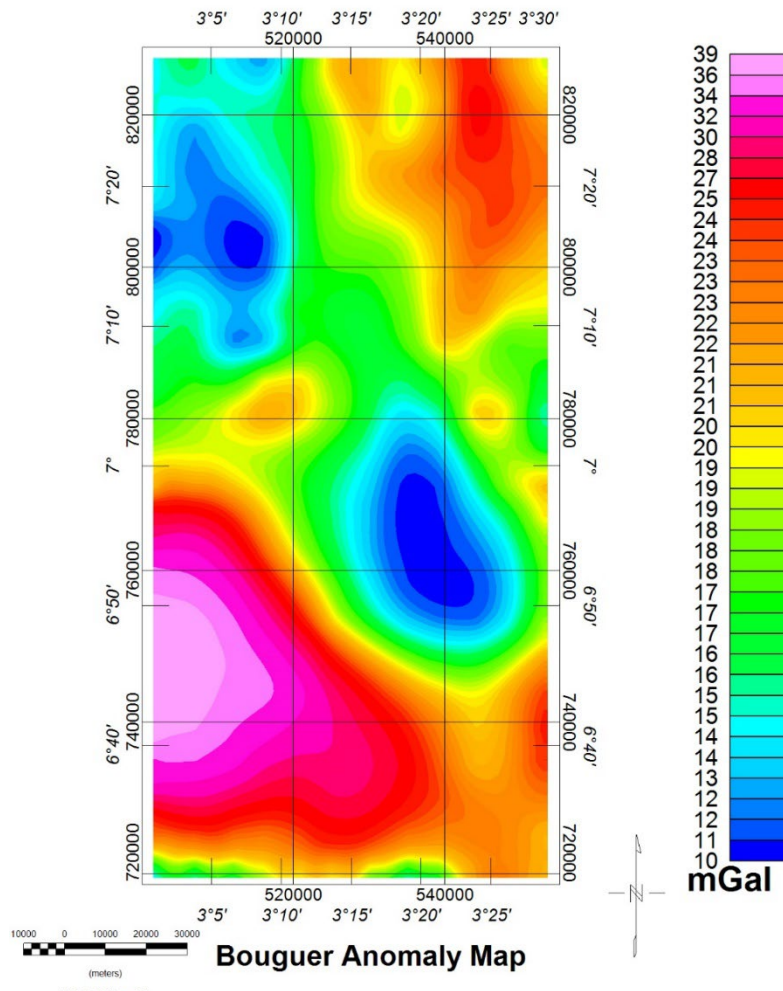


Figure 2. Bouguer anomaly map of the study area.

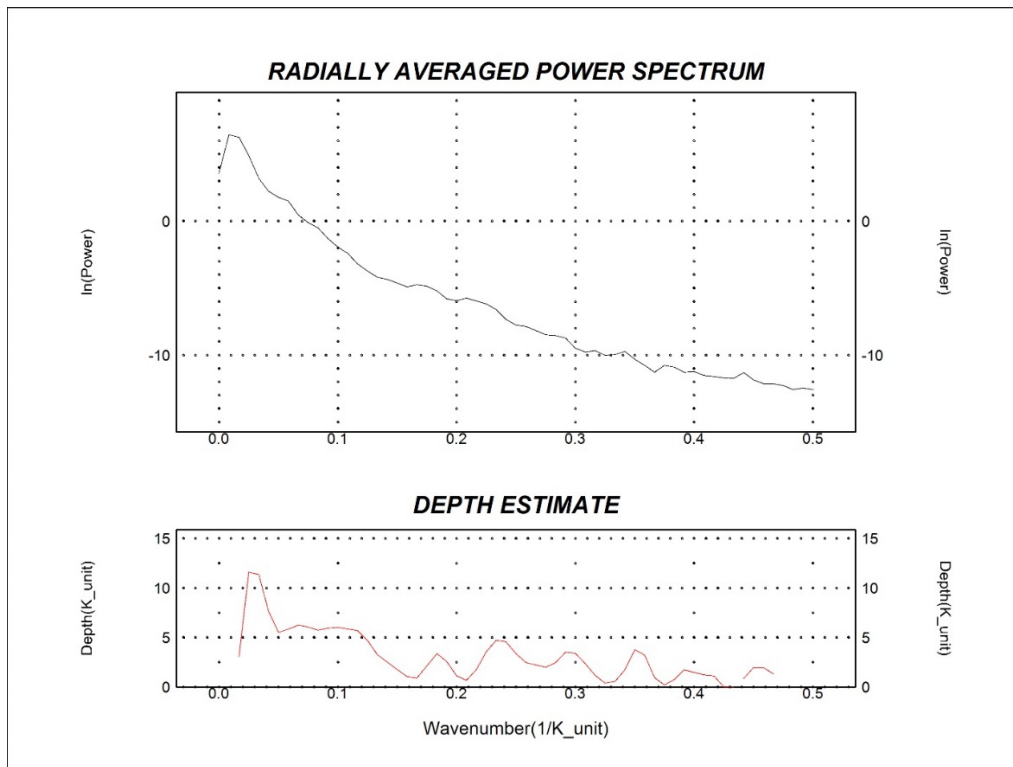


Figure 3. Radially averaged power spectrum.

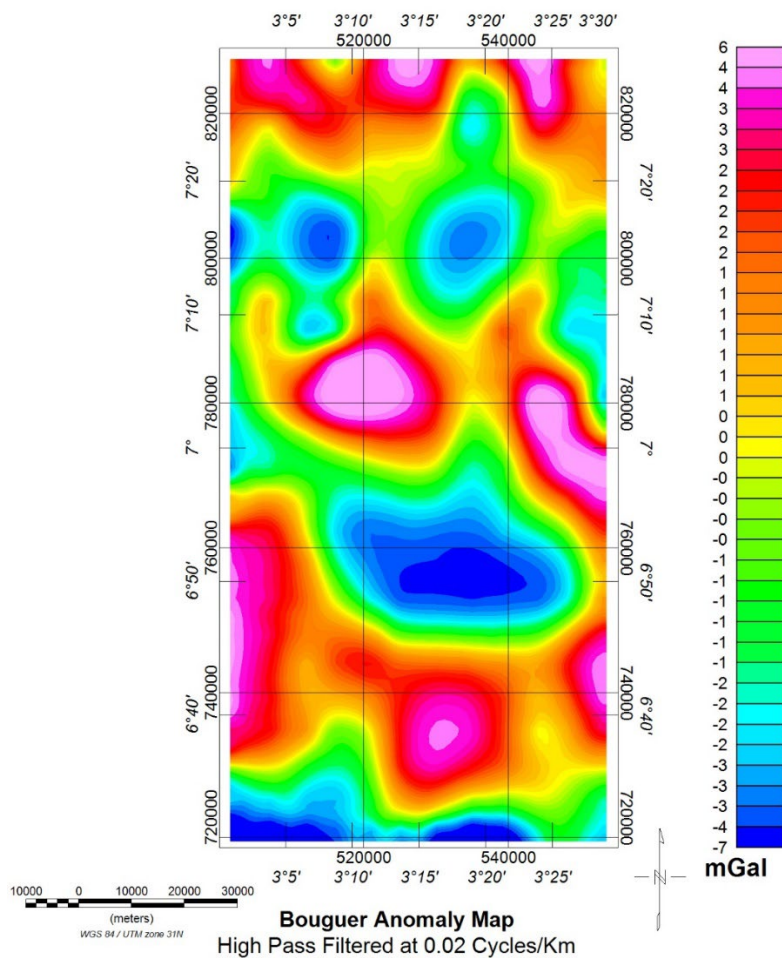


Figure 4. Bouguer anomaly map filtered at 0.02 cycles/km.

A high-pass filter was used to eliminate low frequency anomalies from the gravity field as a whole at 0.02 cycles/km. The cut-off points are visible in the spectrum. The spectrum graph shows the wavenumber (frequency) against the log of the power or data amplitude or the strength of the spectral components. The resulting radially averaged spectrum, which is the pointer suggesting 0.02 cycles/km, can be used to evaluate data contributions. The filter was used to remove long wavelength anomalies as shown in Figure 4. At the extreme north and south of the study area, the Bouguer anomaly map (Figure 4) has areas predominantly marked with high (pink) Bouguer anomaly with depth range from 2 mGal to 6 mGal trending east to west. The low gravity anomaly (blue) is concentrated at the center of the study area with little patches spanning NE to NW and SS of the study area with depth range from -7 mGal to -2 mGal.

4-2 Derivative filtering

Derivative filters are important in the sharpening of edges of anomalies and in enhancing subsurface features associated with shallow anomaly sources. The main objective of its application was to identify near-surface intrusive rocks that could potentially be the targeted shallow-seated gravity signal in the research area. A two-dimensional Fast Fourier Transform (2-D FFT) filtering technique known as MAGMAP was employed in computing the different derivative grids using a systematic filtering process. These grids were produced to further the interpretation of geologic and other linear

structures such as lineaments as contained in the horizontal and vertical derivative maps (Figs. 5-7). The derivative map is a high-pass filter that shows the vertical and horizontal variations in gravitational field with respect to the depth.

Figure 5 shows a horizontal displacement of bodies in the field; the gravitational field ranges from -0.00134 mGal/m to 0.00109 mGal/m with high gravity dominant at the northwest, northeast and southern part of the investigated area. The first horizontal derivative map along y-direction (Figure 6) shows a horizontal displacement of source in the field; the gravitational field ranges from -0.00146 mGal/m to 0.00203 mGal/m with high gravity concentration at the north, central and southern part of the map. The first horizontal maps comprise of a closely packed and loosely-spaced anomaly which could possibly denote the fault zones and lineaments in the area under investigation. The lineaments serve to house the economic deposits, such as limestone, shale, alluvial deposit and the likes. The first vertical map has an anomaly range of -0.00246 mGal/m to 0.00210 mGal/m with high gravity source registered at the north, central and some parts of southern zone of the study area and low gravity field that ranges from -0.00246 mGal/m to -0.00038 mGal/m.

In Figs. 8-11, the interpolated Bouguer gravity and derivative grids of Ewekoro are presented. The low resolution obtained from the gravity grids is a factor of line spacing used in obtaining the aerogravity data which are farther apart.

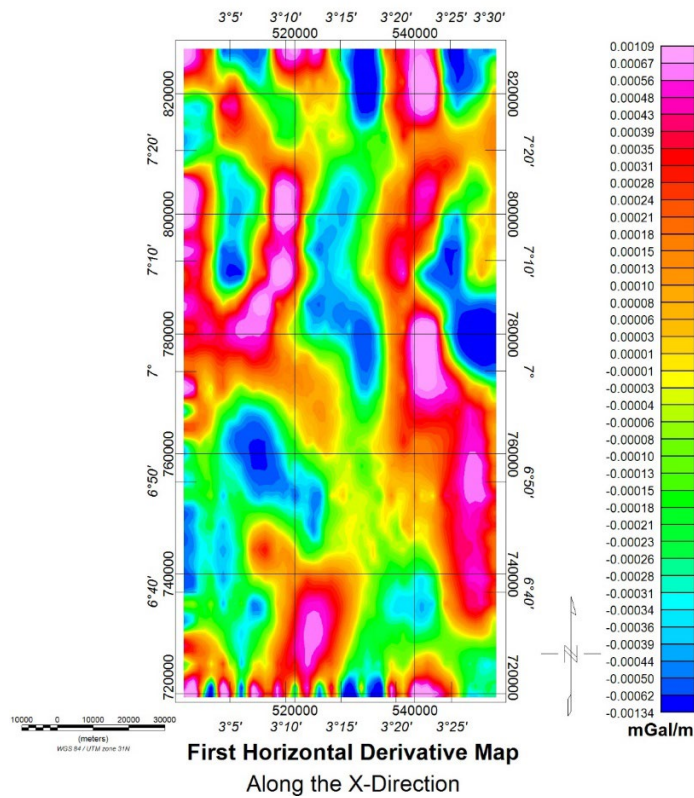


Figure 5. First horizontal derivative map of the Ewekoro sheet along the X-direction.

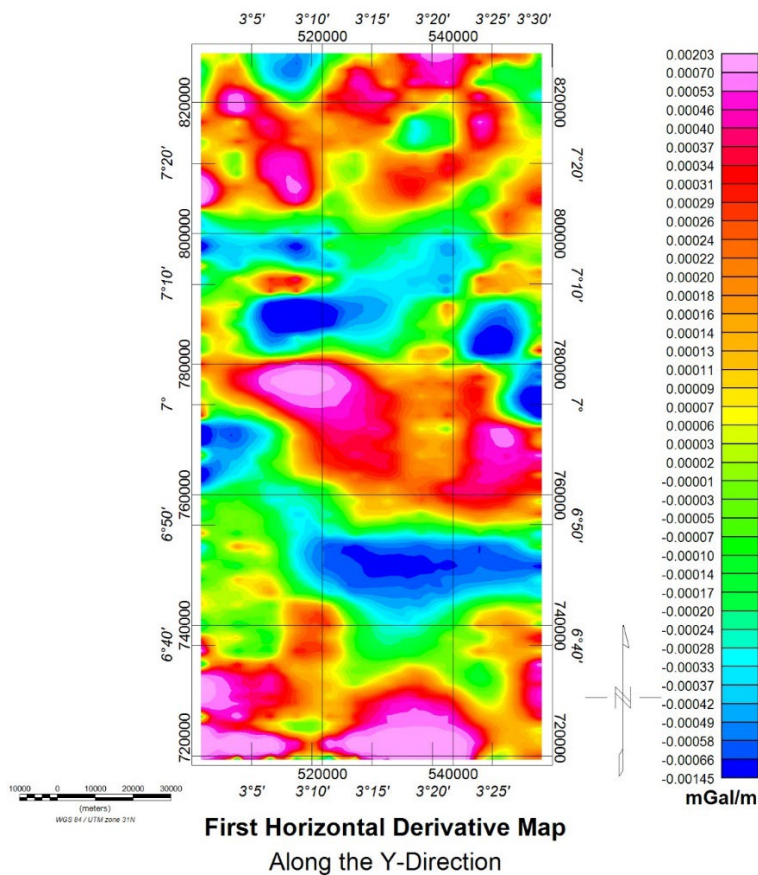


Figure 6. First horizontal derivative map of the study area along the Y-direction.

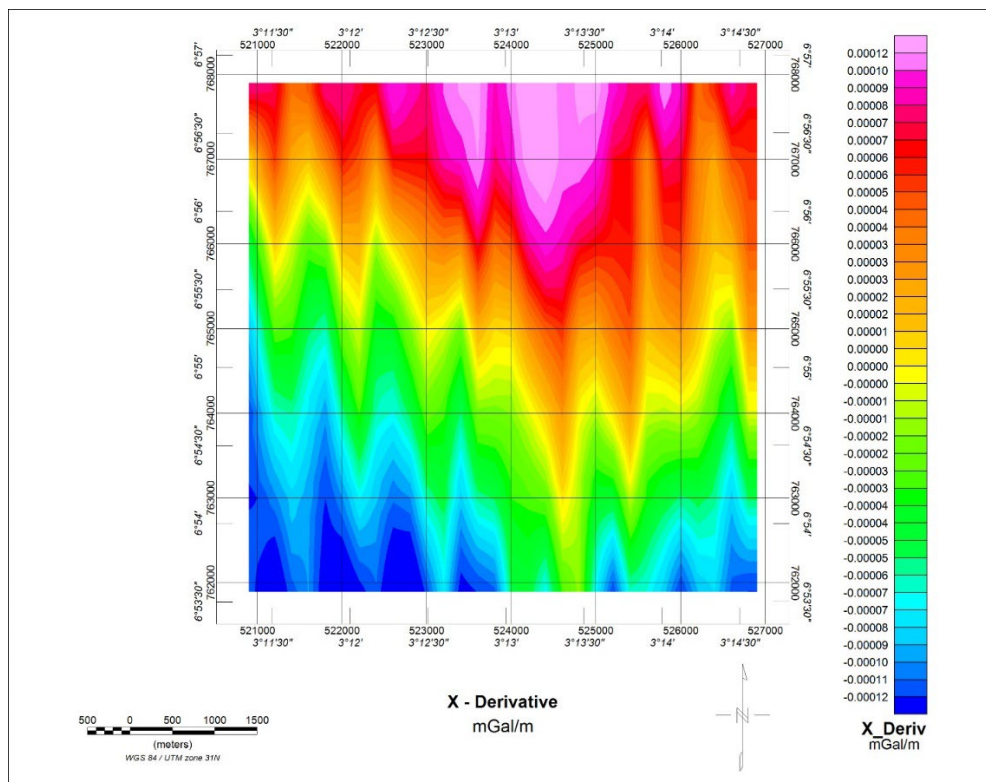


Figure 9. The interpolated gravity map (X-Derivative).

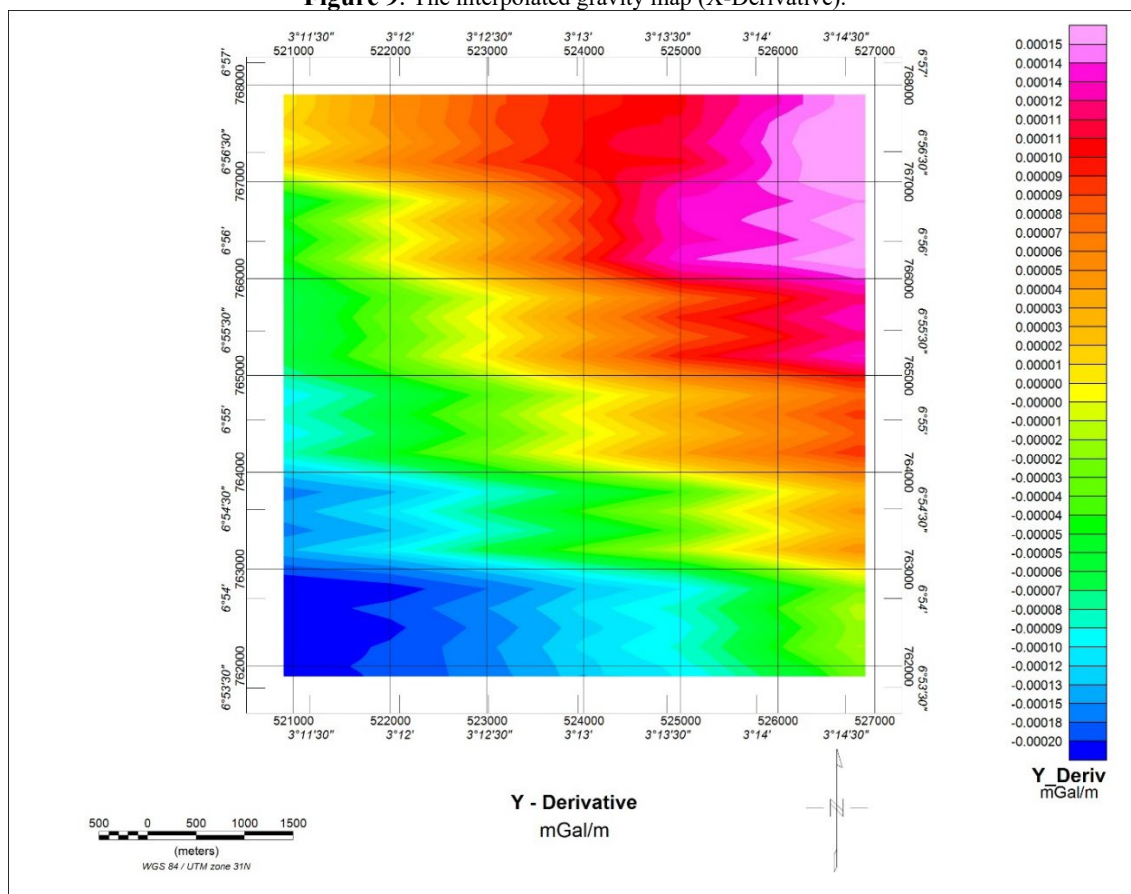


Figure 10. The interpolated gravity map (Y-Derivative).

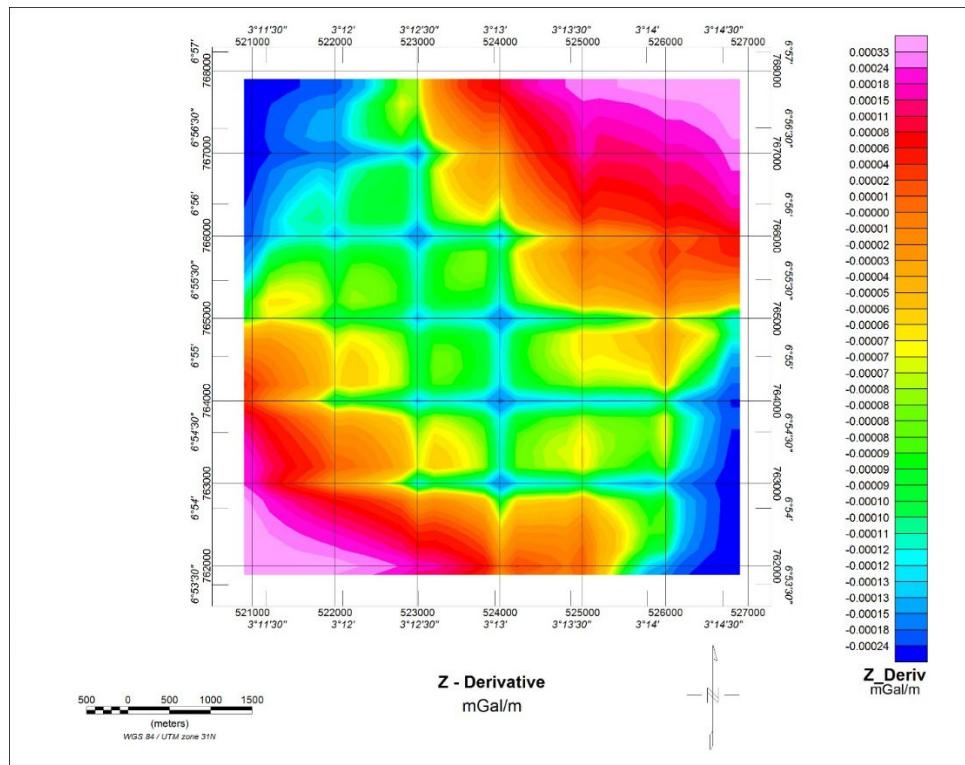


Figure 11. The interpolated gravity map (Z-Derivative).

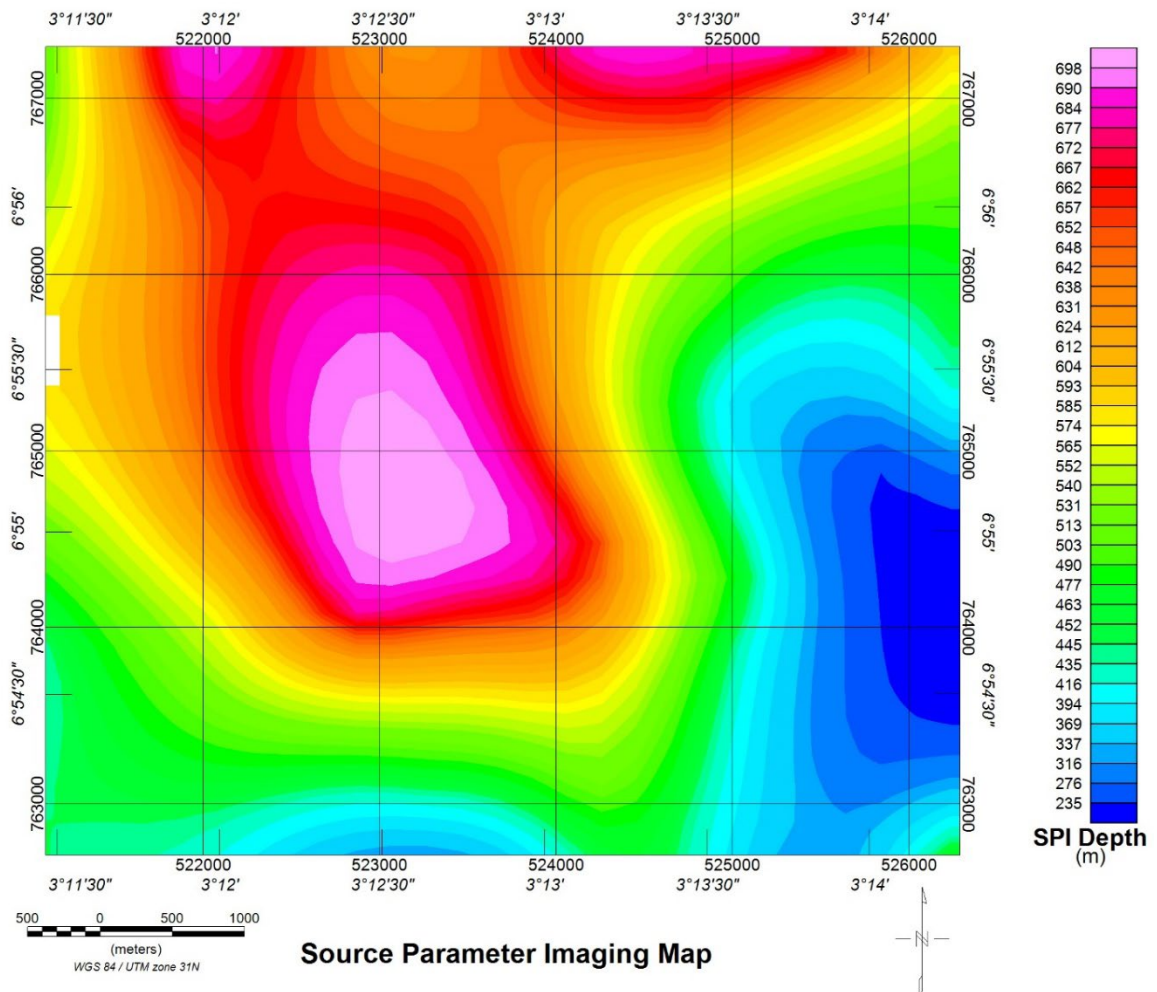


Figure 12. The interpolated SPI map of Ewekoro gravity.

The depth to basement of gravity sources of Ewekoro interpolated is presented in the Source Parameter Imaging (SPI) map of Figure 12. The depth range obtained is at a range of 235 m–698 m. The deeper gravity sources possibly indicate a significant concentration in the central part of the study area (pink and red regions) while the shallower sources are concentrated in the SE of the investigated area. The sources are gravity responses brought on by changes in density contrast.

4-3 3D Euler deconvolution

According to Reeves (2005), the Euler deconvolution method gained a broad application in varying the structural index of the potential field as applied to gridded data. The rate at which the potential field falls off with the distance from a

particular anomaly source related with its gradient component is a function that is measured by the structural index.

Figure 13 presents the Euler map of Ewekoro for SI=0 which can be quantitatively interpreted as having a maximum depth range of 658 m–692 m with an average maximum depth to basement of 675 m, while the minimum depth estimation range was 97 m–134 m with average minimum depth to basement of 115.5 m. At structural index number SI = 0, fault-like or contact-like anomaly is deconvoluted and the Euler solution revealed faults or contact of moderate anomaly trending SSW of the area under investigation. However, the plot revealed a scattered solution in NW, NE and SSE part of the study area, an indication that the geometry of the anomaly is not majorly contacts nor faults.

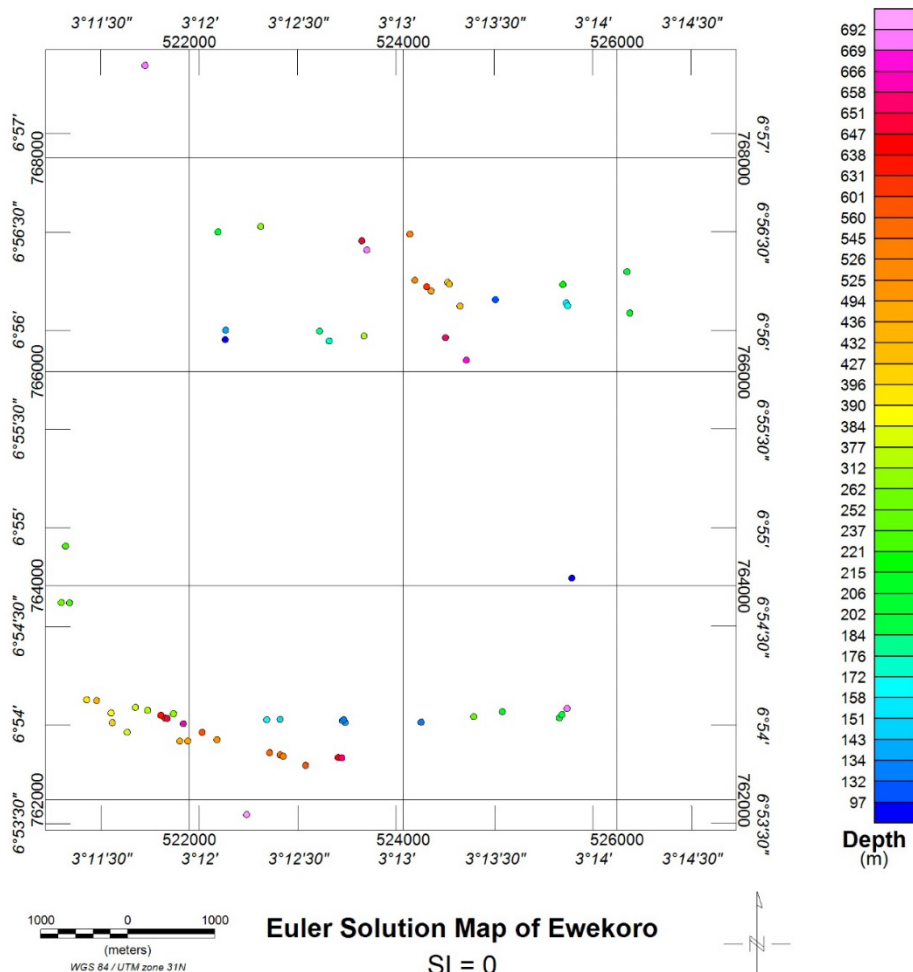


Figure 13. Euler solutions map of Ewekoro interpolated (SI = 0).

5 Conclusion

This study interpreted Bouguer anomaly qualitatively and quantitatively using Source Parameter Imaging and Euler deconvolution from the airborne gravity data of sheets 260 and 279. The data was utilized in determining the dimensions and parameters of gravity anomalies. The gravity data was filtered to attenuate regional effects using the high-pass filter. The qualitative analysis showed that the research area has varied densities that may be caused by sedimentary intrusion into the basement formation, suggesting the potential for the deposit of lower density bodies such as limestone, shale, alluvial deposits, sandstone, and the likes (Layade et al., 2021a). The derivatives map was used to determine the boundaries of the Bouguer anomaly and revealed possible geologic boundaries. Representing the best clustering for 3D Euler solutions, the depth estimates which corresponds to $SI = 0$ revealed a depth estimate of 97 m to 692 m, while the SPI revealed a depth estimate of 235 m–698 m. The depth estimate obtained from the windowed grids using the SPI and 3D Euler deconvolution methods are 235 m–698 m and 97 m–692 m, respectively, indicating a depth broad range of 97 m–698 m (Layade et al., 2020). The qualitative interpretation of the data showed that there exists heterogeneity of distribution of gravity field source in the study area which could be due to lateral orientation of anomaly source in the north to south zone. Conclusively, the overburden thickness of Ewekoro trends in the NNE–NNW with an appreciable depth to harbour mineral resources.

Acknowledgment

The authors appreciate the Bureau Gravimetrique International (BGI), through the Earth Gravity Model (EGM08) in 2008 for the available of the data sets used in the work.

References

- Adegoke, J. A., and Layade, G. O., 2019, Comparative depth estimation of iron-ore deposit using the data-coordinate interpolation technique for airborne and ground magnetic survey variation: African Journal of Science, Technology, Innovation and Development, **11**(5), 663-669, doi:10.1080/20421338.2019.1572702.
- Adejuwon, J. O., and Adelakun, M. A., 2012, Physiochemical and bacteriological analysis of surface water in Ewekoro local government area of Ogun State Nigeria, A case study of Lala, Yobo and Agodo Rivers: International Journal of Water Resources and Environmental Engineering, **4**, 66-77.
- Bonde, D. S., Udensi, E. E., and Momoh, M., 2014, Modeling of magnetic anomaly zones in Sokoto Basins, Nigeria: IOSR Journal of Applied Geology and Geophysics, **2**(1), 19-25.
- Jones, H. A., and Hockey, R. D., 1964, The geology of part of southwestern Nigeria: Geological Survey of Nigeria Bulletin, **31**(39), 1-101.
- Kearey, P., Brooks, M., and Hill, I., 2002, An Introduction to Geophysical Exploration: Blackwell Science Ltd, third edition, 12-148.
- Layade, G. O., Edunjobi, H. O., Ajayi, K. D., and Olujimi, D. P., 2021a, Ground based gravimetric for the detection and depth mapping of subsurface geological features: Journal of the Earth and Space Physics, **46**(4), 159-171, doi: 10.22059/jesphys.2020.301010.1007209.
- Layade, G. O., Edunjobi, H. O., Makinde, V., and Bada, B. S., 2021b, Application of forward and inverse modelling to high-resolution gravity data for mineral exploration: Journal of the Earth and Space Physics, **46**(4), 117-129,

- doi:10.22059/jesphys.2020.296560.1007192.
- Layade, G. O., Edunjobi, H. O., Makinde, V., and Bada, B. S., 2020, Estimation of depth to Bouguer anomaly sources using source parameter imaging and Euler deconvolution techniques in basement complex-sedimentary formation: *RMZ Materials and Geoenvironment*, **67**(4), 185-195, doi:10.2478/rmzmag-2020-0016.
- Nabighian, M. N., 1972, The analytic signal of 2D magnetic bodies with polygonal cross sections: its properties and use for automated anomaly interpretation: *Geophysics*, **37**, 507–517.
- Nabighian, M. N., Ander, M. E., Graunch, V. J. S., et al., 2005, 75th Anniversary - Historical development of gravity method in exploration: *Geophysics*, **70**(6), 63ND–89ND, doi:10.1190/1.2133785.
- Ngozi, A. O., Ezemnah, K. C., and Igwe, E. A., 2019, Euler deconvolution and source parameter imaging of aeromagnetic data of Guzabure and Gudumbali regions, Chad Basin, North Eastern Nigeria: *IOSR Journal of Applied Physics (IOSR-JAP)*, **11**(3), 1-10.
- Nwosu, O. B., 2014, Determination of magnetic basement depth over parts of middle Benue trough by Source Parameter Imaging (SPI) technique using HRAM: *International Journal of Scientific and Technology Research*, **3**(1), 262-271.
- Oladosu, Y. C., and Ogundipe, O. Y., 2017, Micropaleontological studies of Ewekoro sediments Southwestern Nigeria: *Journal of Geology and Geophysics*, **6**, 280, doi:10.4172/2381-8719.1000280.
- Oli, I. C., Okeke, O. C., Abiahu, C. M. G., Anifowose, F. A., and Fagorite, V. I., 2019, A review of the geology and mineral resources of Dahomey Basin, Southwestern Nigeria: *International Journal of Environmental Sciences & Natural Resources*, **21**(1), 556055, doi:10.19080/IJESNR.2019.21.556055.
- Olurin, T. O., Badmus, B. S., Akinyemi, O. D., Olowofela, J. A., Ozebo, V. C., and Ganiyu, S. A., 2012, Analysis of physical parameters of limestone deposits in Ewekoro formation, Southwestern Nigeria: *Earth Science Research*, **1**(2), 1927-0550.
- Osazuwa, I. B., 2014, Non-seismic methods applied to oil and gas industry: Lectures delivered at the Centre of Excellence in Geosciences and Petroleum Engineering at the University of Benin, Nigeria.
- Reid, A. B., Allsop, J. M., Granser, H., Millet, A. J., and Somerton, I. W., 1990, Magnetic interpretation in three dimensions using Euler deconvolution: *Geophysics*, **55**, 80–91.
- Reid, A. B., Ebbing, J. O., and Susan, S. J., 2014, Avoidable Euler errors—the use and abuse of Euler deconvolution applied to potential fields: *Geophysical Prospecting*, **62**, 1162-1168, <https://doi.org/10.1111/1365-2478.12119>.
- Revees, C., 2005, *Aeromagnetic Surveys: Principles, Practice & Interpretation: GEOSOFT*.
- Reynolds, J. M., 1997, *An Introduction to Applied and Environmental Geophysics: John Wiley and Sons, NY*.
- Rivas, J. A., 2009, Gravity and magnetic methods: Short course on surface exploration for geothermal resources: Organized by UNU-GTP and La Geo, in Ahuachapan and Santa Tecla, El Salvador, 17-30 October 2009.
- Sheriff, R. E., 2002, *Encyclopedic Dictionary of Applied Geophysics: Society of Exploration Geophysics*.
- Stavrev, P., and Reid, A., 2007, Degrees of homogeneity of potential fields and structural indices of Euler deconvolution: *Geophysics*, **72**(1), L1–L12.

Thompson, D. T., 1982, A new technique for making computer-assisted depth estimates from magnetic data: *Geophysics*, **47**(1), 31–37.
Thurston, J. B. and Smith, R. S., 1997,

Automatic conversion of magnetic data to depth dip and susceptibility contrast using the SPI methods: *International Journal of Geophysics*, **62**(3), 807–813.